

Janus nanoparticles: reaction dynamics and NOESY characterization

Sulolit Pradhan · Lauren E. Brown ·
Joseph P. Konopelski · Shaowei Chen

Received: 1 August 2008 / Accepted: 18 October 2008 / Published online: 14 November 2008
© Springer Science+Business Media B.V. 2008

Abstract Janus nanoparticles were prepared by taking advantage of interfacial ligand exchange reactions of hydrophobic hexanethiolate-protected gold nanoparticles with hydrophilic 2-(2-mercaptoethoxy)ethanol (MEA). A monolayer of the particles was first formed at the air–water interface by the Langmuir technique and then deposited onto a substrate surface by the Langmuir–Blodgett method. The particle monolayer was then immersed into an aqueous solution of MEA for different periods of time. It was found that the exchange reactions occurred but were limited only to the top face of the nanoparticles and the reaction reached equilibrium in about 8 h. The resulting particles exhibited amphiphilic characters as confirmed by contact angle and UV–visible, FTIR and NMR spectroscopic measurements. Of these, the structural discrepancy between the Janus nanoparticles and bulk-exchanged particles was clearly manifested, in particular, by NOESY NMR measurements.

Keywords Janus nanoparticles ·
Langmuir–Blodgett · Contact angle · NOESY NMR ·
Surface plasmon · Exchange reactions · Monolayer

Introduction

Recently, nanoparticle materials with asymmetric chemical/physical properties or geometric structures have attracted much interest because of their unique performance that cannot be achieved by the homogeneous or symmetric counterparts. In particular, the formation of functional nanoarchitectures via controlled self assembly and the resulting wide range of possible applications in science and technology can be approached via asymmetric structures most efficiently (Feldheim et al. 1996; Storhoff et al. 1998; Ujihara et al. 2006; Whetten et al. 1996; Zhang and Cui 1998). Of these, spherical nanoparticles with two structurally and functionally asymmetric hemispheres, often referred to as Janus nanoparticles, are of significant interest as they are anticipated to behave as nanoscale analogs to conventional amphiphilic surfactant molecules (van Herikhuyzen et al. 2008). In recent years, significant attention has been paid to Janus-type materials because of their potential applications in dual-functional devices (Perro et al. 2005), structural materials for organized assembly (Glotzer 2004; Nie et al. 2006), electronic paper and display applications (Nisisako et al. 2006), surfactants for emulsion systems (Binks et al. 2006), anisotropic imaging probes for both diagnostic and therapeutic purposes, bimetallic nanomotors (Wang et al. 2006b), nanoprobcs (Takei and Shimizu 1997), and anisotropic plasmon materials (Wang et al. 2006a).

S. Pradhan · L. E. Brown · J. P. Konopelski ·
S. Chen (✉)

Department of Chemistry and Biochemistry, University of
California, 1156 High Street, Santa Cruz, CA 95064, USA
e-mail: schen@chemistry.ucsc.edu

In our previous work (Pradhan et al. 2007; Xu et al. 2007), we developed an effective approach based on interfacial engineering for the preparation of Janus gold nanoparticles. First, a monolayer of hexanethiolate-protected gold nanoparticles was formed at the air–water interface by the Langmuir technique. The particle monolayer was then compressed to a selected surface pressure where ligand intercalation between adjacent particles occurred such that the interfacial mobility of the nanoparticles was impeded. A calculated amount of hydrophilic thiol derivatives (1,2-mercaptopropanediol, MPD) was then injected into the water subphase, where ligand place-exchange reactions were initiated and limited to the bottom face of the nanoparticle molecules that was in direct contact with water. Consequently, the resulting particles exhibit hydrophobic characters on one side and hydrophilic on the other. The amphiphilic nature of these particles was then confirmed by contact angle and other spectroscopic measurements, and the particles were found to form stable aggregate structures in an appropriate solvent medium.

In the present investigation, we describe a new procedure for the preparation of Janus nanoparticles again by taking advantage of the surface ligand exchange reactions of alkanethiolate-protected gold nanoparticles with another thiol derivative. In this approach, a monolayer of particles is first deposited onto a substrate surface by the Langmuir–Blodgett (LB) technique. The sample is then immersed into an aqueous solution of the hydrophilic ligands, where the ligand-exchange reactions are limited to the top face of the nanoparticles and hence the formation of Janus nanoparticles. With this experimental setup, the exchange dynamics can also be readily assessed by contact angle measurements, which has remained largely unexplored so far.

Additionally, by using a long hydrophilic ligand, 2-(2-mercaptoethoxy)ethanol (MEA) as compared to the short 1,2-mercaptopropanediol (MPD), used in earlier studies (Pradhan et al. 2007; Xu et al. 2007), the structural details of the Janus nanoparticles will be examined by nuclear Overhauser enhancement spectroscopy (NOESY), which we believe is the first of its kind in the investigation of Janus nanoparticles. This is a two-dimensional phase-sensitive NMR technique that detects the distance-dependent nuclear Overhauser effect between proton spins. Since NOESY signals depend inversely on the distance to the sixth power,

only short-range dipolar couplings are resolved, and it is a very useful tool to examine the conformation of molecules. For instance, NOESY NMR spectroscopy has been used extensively in the field of proteomics to investigate micelle interactions (Bella et al. 1999; Emin et al. 2007). It has also been used to evaluate the statistical distribution of polymers as capping materials for semiconductor quantum dots (Guo and Moffitt 2007), and to study the amide proton exchange rates in metal nanoparticles that are capped with amidethiolates (Kohlmann et al. 2001). Thus, in this study, we would employ NOESY NMR spectroscopy to further verify the surface structural asymmetry of the Janus nanoparticles as compared to bulk-exchanged nanoparticles where the ligands are mixed rather homogeneously on the particles, by taking advantage of the different ligand distribution and the consequent ligand–ligand interactions.

Experimental section

Chemicals

Hydrogen tetrachloroauric acid ($\text{HAuCl}_4 \cdot x\text{H}_2\text{O}$) was synthesized by dissolving ultra-high purity gold (99.999%, Johnson Matthey) in freshly prepared aqua regia followed by crystallization (Brauer 1963). Tetraoctylammonium bromide (Alfa Aesar, 98%), hexanethiol (C_6SH , Acros, 96%), and sodium borohydride (NaBH_4 , Acros, 99%) were all used as received. 2-(2-Mercaptoethoxy)ethanol (MEA, $\text{HSCH}_2\text{CH}_2\text{OCH}_2\text{CH}_2\text{OH}$) was synthesized and characterized according to a literature procedure (Woehrle et al. 2004). Other solvents were purchased from typical commercial sources at their highest purity and used without further treatments. Water was supplied by a Barnstead Nanopure water system (18.3 M Ω cm).

Nanoparticle preparation

Hexanethiolate-protected gold (AuC6) particles were synthesized and purified by using the Brust protocol (Brust et al. 1994). These particles then underwent fractionation by using a solvent–nonsolvent mixture of toluene and ethanol (Chen 2001a; Templeton et al. 2000), and the fraction with an average core diameter of 2.0 nm (corresponding approximately to a particle composition of $\text{Au}_{314}\text{C}_{691}$) (Hostetler et al. 1998)

was used for the subsequent study. These particles were then subject to thermal annealing in toluene at 110 °C in an oil bath for 8 h to further reduce the dispersity of the core size and shape (Chen 2001b).

Janus nanoparticles

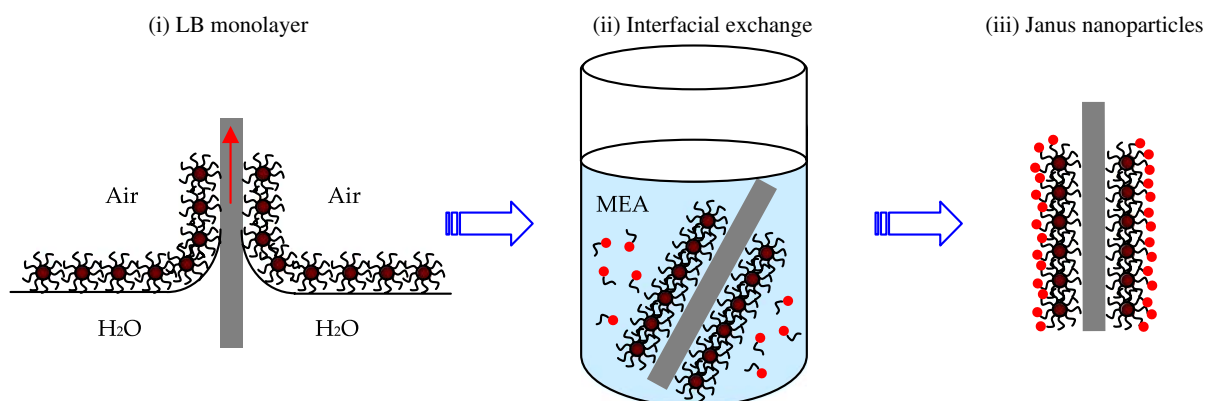
The Janus nanoparticles were then prepared by taking advantage of the partial exchange reactions of the AuC6 particles obtained above with MEA ligands. The procedure was depicted in Scheme 1. First, a monolayer of the AuC6 nanoparticles was formed on the water surface of a Langmuir–Blodgett trough (NIMA Technology, Model 611D). In a typical experiment, 300 μL of the AuC6 particle solution (at a concentration of 0.8 mg/mL in toluene) was spread onto the water surface using a Hamilton microliter syringe. At least 2 h was allowed for solvent evaporation and between compression cycles. The barrier speed was maintained at 10 cm^2/min . The particle monolayer was then compressed to a desired surface pressure where the interparticle edge to edge separation was maintained at a value smaller than twice the extended ligand chain length. This resulted in ligand intercalation between adjacent particles which helped to maintain the structural integrity of the particle monolayers after deposition. At this surface pressure, the particle monolayer was deposited by the Langmuir–Blodgett technique onto a clean glass slide (Step (i)). The surface area of the glass slide was typically 8 $\text{cm} \times 3 \text{ cm}$. The glass substrate with the deposited particle monolayer was then immersed into a water solution of 1 mM MEA that

was kept in a water circulation bath with the temperature set at 45 °C (Step (ii)). It is anticipated that the exchange reactions of the AuC6 particles with the MEA ligands only occur at the top face of the particles that is in direct contact with the water phase, hence the generation of Janus nanoparticles (Step (iii)). At varied immersion time intervals, the glass slide was taken out of the MEA solution, gently rinsed with copious amounts of water and ethanol to remove excessive MEA and displaced hexanethiolate ligands, dried in a gentle stream of ultrahigh-purity nitrogen, and then subject to contact angle measurements before being collected into a vial by chloroform. At least four batches of particle samples were prepared and collected under identical conditions so that there were enough materials for further analyses. The resulting Janus particles were found to be soluble in chloroform and THF.

As a control measurement, exchange reactions of AuC6 nanoparticles with MEA were also carried out by mixing a calculated amount of AuC6 nanoparticles and MEA ligands in THF and stirred for 48 h. The solution was then dried under reduced pressure with a rotary evaporator and excessive ligands were removed by extensive rinsing with methanol. The resulting particles were denoted as bulk-exchange particles, and, similar to the Janus nanoparticles, soluble in THF and chloroform.

Contact angle measurements

Contact angles of nanoparticle thin films were evaluated with a TanteC CAM-PLUS Contact Angle Meter.



Scheme 1 Schematic of the formation of Janus nanoparticles based on interfacial exchange reactions of AuC6 nanoparticles with MEA ligands

For each sample, at least eight independent measurements were carried out for statistical analyses. Prior to deposition, a flat glass substrate was cleansed in aqua regia followed by extensive rinsing with water and ethanol, and blow-dried by ultrahigh-purity nitrogen. The substrate was then cleaned in a UV-ozone chamber (Jelight Model 42) for 15 min to remove any organic contaminants. For the Janus nanoparticles, the contact angle was monitored at different immersion time intervals of the AuC6 particle monolayer immersed in an MEA solution; whereas for the bulk-exchange particles, a monolayer was deposited onto a glass slide surface by the LB technique (the dipper speed was generally controlled at 1 mm/min) in both the upstroke and downstroke configurations, and their contact angles were then measured and compared.

Spectroscopy

FTIR measurements of the particles were performed with a Perkin–Elmer Precision Spectrum-1 FTIR Spectrometer. The particles were first dissolved in chloroform and a thick film was formed by dropcasting the solution onto a CsBr plate. The sample was then dried in a gentle stream of nitrogen. The UV–visible spectra were collected with a UNICAM ATI UV4 spectrometer at a particle concentration of 0.1 mg/mL in chloroform using a 1 cm quartz cuvette. ^1H and NOESY NMR spectra were collected by using a VARIAN OXFORD 600 MHz spectrometer. The particles were dissolved in CDCl_3 at a concentration of 1 mg/mL. Dynamic light scattering (DLS) measurements were carried out with a ProteinSolution *Dynapro* Temperature Controlled Microsampler. Typically an aliquot (12 μL) of the particle solutions at a concentration of 0.05 mg/mL in THF was introduced into a sample holder using a 20 μL micropipette. The results were reported in terms of %mass.

Results and discussion

In our previous studies (Pradhan et al. 2007; Xu et al. 2007), Janus nanoparticles were prepared by the exchange reactions of hydrophobic AuC6 nanoparticles with 1,2-propanediol (MPD) at the air–water interface. However, with MEA ligands, it is somewhat puzzling and surprising that this procedure was not very effective. Thus, a different synthetic scheme

was designed as depicted in Scheme 1, where the Janus nanoparticles were produced by taking advantage of the interfacial exchange reactions of the nanoparticle LB monolayers with hydrophilic thiol derivatives.

To authenticate the amphiphilic nature of the resulting Janus nanostructures, a series of characterizations were carried out. First, the contact angle of the nanoparticle LB monolayers was evaluated at different immersion time intervals (Step (ii)), which is shown in Fig. 1. It can be seen that for the AuC6 particle layers (i.e., $t = 0$), the contact angle is $59.1^\circ \pm 1.0^\circ$. Interestingly, within the first 5 h of immersion of the particle monolayer into the MEA aqueous solution, the contact angle remains virtually unchanged. It then decreases slightly to $56.1^\circ \pm 1.8^\circ$ at $t = 6$ h; whereas at $t = 8$ h, it drops rather drastically to $49.0^\circ \pm 1.3^\circ$ and remains practically (statistically) invariant thereafter (up to 32 h). It has been found previously that because of the nanocrystalline morphology of the nanoparticles, ligand place-exchange reactions on alkanethiolate-protected gold nanoparticles most likely start with the surface defect sites and then propagate to the terrace sites (Guo et al. 2005; Hostetler et al. 1999; Song and Murray 2002). Thus, the observed evolution of the contact angle of nanoparticle LB monolayers with immersion time is anticipated to reflect the reaction dynamics. That is, the small decrease of contact angle within the first 5 h is a consequence of the initial phase of exchange reactions involving surface defects, whereas the more significant drop of contact angles

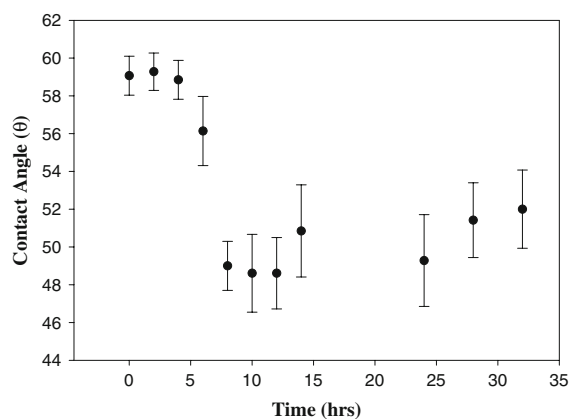


Fig. 1 Contact angle of a Langmuir–Blodgett monolayer of AuC6 nanoparticles after being immersed in 1 mM MEA in water at 40 °C for different periods of time

at 8 h actually arises from the incorporation of hydrophilic MEA ligands onto the more populous terrace sites on the particle surface. The almost constant contact angle after 8 h seems to suggest that the exchange reaction has reached equilibrium. This may be accounted for by the inaccessibility of the bottom face of the nanoparticles by the MEA ligands because of ligand intercalation which leads to impeded interfacial mobility of the nanoparticles on the substrate surface. In fact, experimentally we observed no apparent loss of nanoparticles into the water solution during the entire experimental procedure, which implies that not all the original protecting ligands (hexanethiolates) were replaced by the MEA ligands.

Note that for bulk-exchange nanoparticles, the contact angle of the particle monolayer deposited by the LB technique is $55.8^\circ \pm 2.0^\circ$, which falls into the intermediate between that of the AuC6 nanoparticles and the Janus nanoparticles. Such a behavior was also observed earlier in the preparation of Janus nanoparticles based on MPD exchange (Pradhan et al. 2007; Xu et al. 2007). Comparison with two-dimensional self-assembled monolayers (2D SAMs) of varied thiol derivatives formed on flat gold film surfaces further confirms the asymmetric structure of the Janus nanoparticles. For instance, for 2D SAM of hexanethiols, the contact angle is $63.1^\circ \pm 3.4^\circ$, which is close to that of the LB monolayers of the original AuC6 nanoparticles (Fig. 1); for MEA monolayers, it is $47.8^\circ \pm 2.7^\circ$, very similar to that of the hydrophilic face of the Janus nanoparticles (e.g., Fig. 1); and for the mixed monolayer of hexanethiol and MEA, it becomes $53.2^\circ \pm 2.2^\circ$, which is consistent with that observed above with the bulk-exchange nanoparticles, suggesting a rather similar homogeneous mixing of the two mercapto-derivatives on the substrate surface.

To further verify the incorporation of the MEA ligands onto the particle surface, FTIR measurements were performed on the Janus, bulk-exchanged, and AuC6 nanoparticles. Figure 2 shows the respective spectrum. It can be seen that the most prominent change with respect to the AuC6 particles is the appearance of a broad peak centered at $3,400\text{ cm}^{-1}$ and another at $1,125\text{ cm}^{-1}$ for the Janus and bulk-exchanged particles. The former may be ascribed to the O–H vibrational stretch of the MEA ligands, whereas the latter is most probably due to the

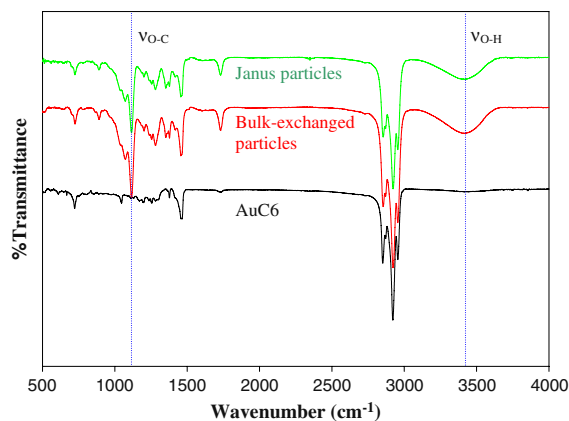


Fig. 2 FTIR spectra of the AuC6, bulk-exchanged, and Janus nanoparticles

asymmetrical C–O–C stretch. Both features suggest the successful exchange of MEA onto the nanoparticle surface.

Consistent results were also obtained in UV–Vis spectroscopic study. Figure 3 depicts the optical absorption profiles of the (a) AuC6, (b) bulk-exchanged, and (c) Janus nanoparticles in different solvent media. It can be seen that in panel (a), because of the small size, the AuC6 particles exhibited an exponential decay profile in THF due to Mie scattering, along with a weak and broad peak at 520 nm that is the characteristic surface plasmon resonance (SPR) of nanosized gold particles (Bohren and Huffman 1983; Kerker 1969). Similar behaviors were observed with the bulk-exchanged nanoparticles in THF (solid curve in panel (b)); whereas in the THF:water mixture (v:v 1:1), the SPR peak becomes slightly better defined (with a small increase of the peak intensity), suggestive of particle aggregation in this solvent medium, most probably because of the homogeneous distribution of the hydrophobic and hydrophilic ligands on the particle surface which renders it difficult for the particles to orient themselves to minimize surface energy (dashed curve in panel (b)). In sharp contrast, the SPR peak for the Janus nanoparticles are significantly more pronounced in both water and THF:water mixture (v:v 1:1), as manifested in panel (c) by the solid and dashed curves, respectively. This suggests extensive aggregation of the nanoparticles in these two solvent media, where the amphiphilic nature of the particle surface allows for particle organized assembly so that the surface energy would be minimized. The overall

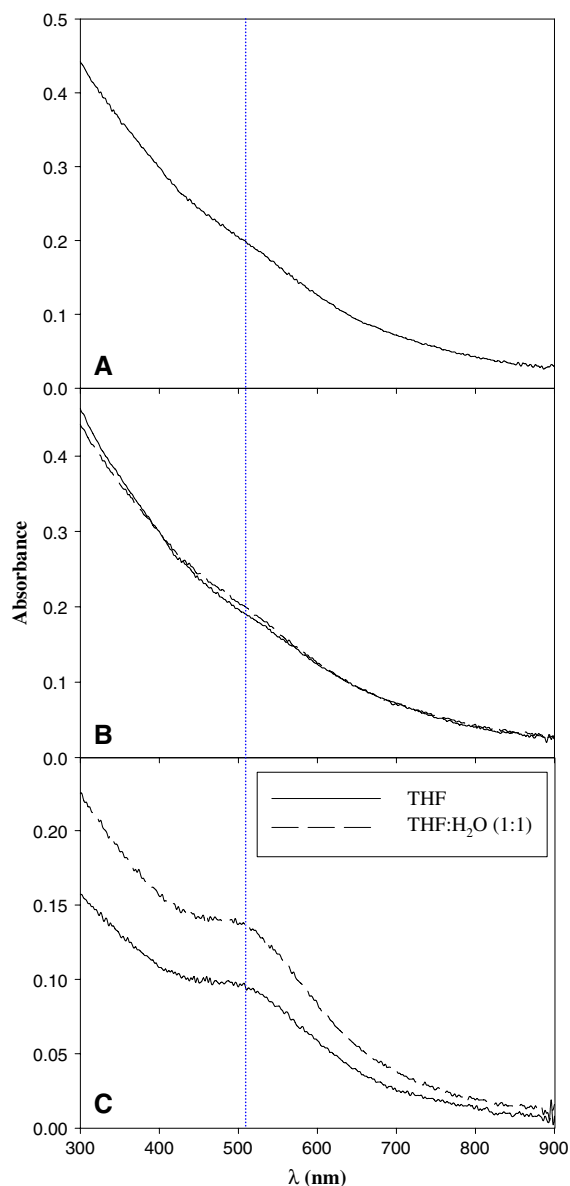


Fig. 3 UV-Vis spectra of different nanoparticles: **a** AuC6 particles, **b** bulk-exchanged particles, and **c** Janus nanoparticles. Solid curves are for particles dissolved in THF and dashed curves are for particles in a (v:v 1:1) mixture of THF and water. All particle concentrations 1 mg/mL in the respective solvent

behaviors are very analogous to what we observed earlier with the MPD-based Janus nanoparticles (Pradhan et al. 2007; Xu et al. 2007).

The aggregation of nanoparticles in these solvent media was further verified by DLS measurements in THF. For the AuC6 nanoparticles, the average radius

was 1.9 nm. Considering the nanoparticle core diameter of ca. 2 nm and the fully extended chain length of the hexanethiolate ligand of 0.77 nm, this is in good agreement with the particle physical diameter and hence indicative of isolated nanoparticles in the solution. For the bulk-exchanged nanoparticles, the DLC radius is 11 nm whereas for the Janus nanoparticles, 77 nm. Again, these results suggest different degrees of particle aggregation and are consistent with the UV-vis data shown above (Fig. 3).

For a quantitative assessment of the surface composition and ligand distribution of the Janus and bulk-exchanged nanoparticles, NMR spectroscopic measurements were carried out. Figure 4 (a, top) depicts a representative ^1H NMR spectrum of the Janus nanoparticles in CDCl_3 . The peak at 0.90 ppm is ascribed to the protons of the terminal methyl group of the hexanethiolate ligands, whereas the broad peaks at 3.60 and 3.80 ppm are attributable to the methylene protons next to the hydroxyl group and the ether group in the MEA ligands, respectively. From the ratio of the integrated peak areas of these protons, it can be estimated that 44.6% of the original hexanethiolate ligands were replaced by MEA ligands in the Janus particles (corresponding to a molecular composition of $\text{Au}_{314}\text{C}_{650.5}\text{MEA}_{40.5}$). In a similar fashion, for the bulk-exchanged particles, the protecting monolayer was found to consist of 51.2% MEA and 48.8% hexanethiolate (panel (b), top, where the molecular composition can be approximated as $\text{Au}_{314}\text{C}_{644.4}\text{MEA}_{46.6}$). Both results suggest an approximately equal number of hydrophobic and hydrophilic ligands on the nanoparticle surface.

Additionally, to further establish the Janus character of the MEA modified nanoparticles, nuclear Overhauser effect spectroscopy (NOESY) was employed to examine the spatial correlation between nuclear spins (Guo and Moffitt 2007; Kohlmann et al. 2001). NOESY is a two-dimensional NMR technique where cross peaks arise from dipole-dipole interactions (i.e., through-space coupling) between nuclear spins that are in close proximity (typically <0.4 nm), as the intensity of the cross peaks depends inversely on the sixth power of the distance between the protons (Morris et al. 2005). These unique features can thus be exploited for an estimation of the internuclear distance, and for monolayer-protected nanoparticles, a quantitative assessment of the packing (distribution) of ligands on particle surfaces. For

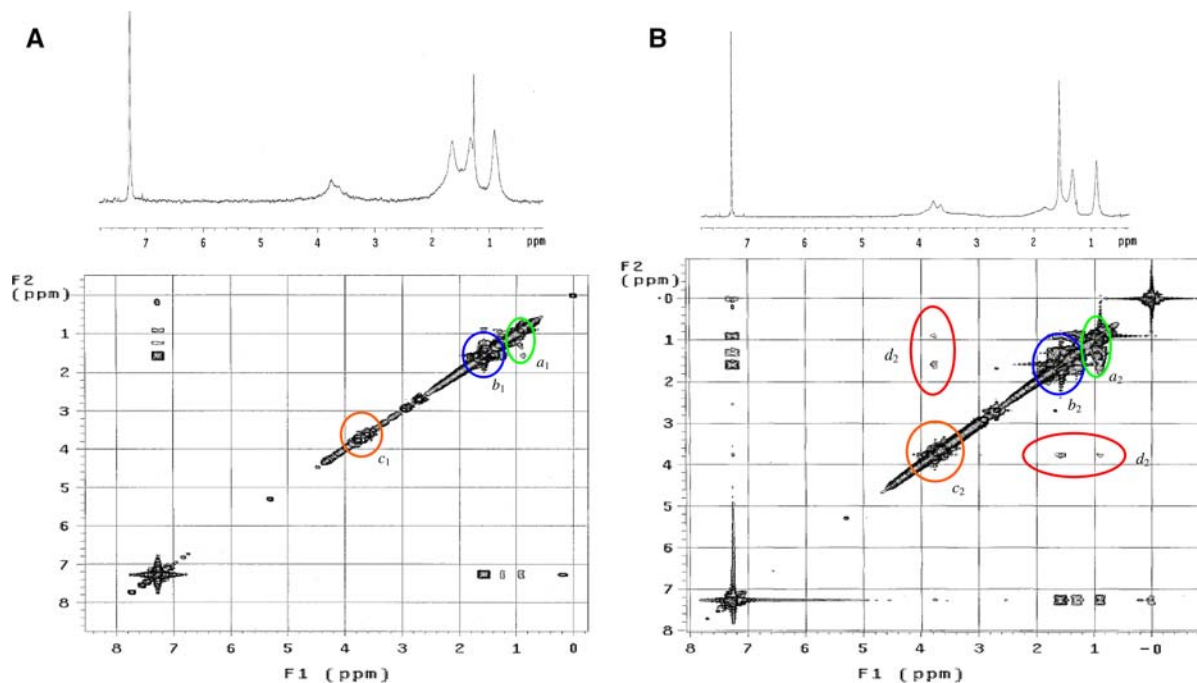


Fig. 4 The ^1H (top panel) and NOESY (bottom panel) NMR spectra of **a** the Janus and **b** bulk-exchanged nanoparticles in CDCl_3 . The corresponding NOESY NMR spectra were

acquired with a mixing time of 120 ms. Circles highlight the cross peaks between the protecting ligands on the particle surface

instance, a recent study by the Murray and Johnson groups (Kohlmann et al. 2001) has demonstrated that NOESY could be used as a powerful tool in the examination of the packing of tiopronin ligands ($\text{CH}_3\text{-CH}(\text{SH})\text{-CO-NH-CH}_2\text{-COOH}$) on gold nanoparticle surfaces by analyzing the cross peaks between the methyl and methylene protons. Since the *intrachain* distance between these protons exceeds the limit of 0.4 nm, the appearance of the cross peaks is most likely arising from the *interchain* contributions, from which a structural model for the packing of the tiopronin ligands can be built (Kohlmann et al. 2001).

Figure 4 depicts a typical NOESY spectrum for both the (a, bottom) Janus and (b, bottom) bulk-exchanged particles. From the diagonal profiles of both spectra, it can be seen that there are apparent polarization interactions between the methylene protons (highlighted in blue and orange circles of b 's and c 's), which most probably arises from *intrachain* interaction of the individual ligand chains as well as *interchain* interaction between adjacent ligands. Of these, the peak in the blue circle (b_1 and b_2) most likely reflects the contribution from the hexanethiolate ligands

whereas that in the orange circle (c_1 and c_2), from the MEA ligands. In addition, the interactions between the methyl protons, and between methyl and methylene protons of the hexanethiolate ligands are clearly manifested in the spectra (green circles of a_1 and a_2).

In addition to these common features, remarkable discrepancy can also be observed. The most significant difference between these two spectra is the appearance of two cross peaks between the methyl/methylene protons of the hexanethiolate ligands and the methylene protons of the MEA ligands for the bulk-exchanged particles, which are highlighted in red circles (d_2) in panel (b). Note that these cross peaks are totally absent in the Janus particles (panel (a)). Such an observation is consistent with the structural models for the surface distribution of the two types of ligands on the nanoparticle surface. In the Janus nanoparticles, the absence of these cross peaks clearly indicates that the hexanethiolate ligands are situated far away from the MEA ligands, because of the segregated distribution of these two ligands on two different hemispheres of the nanoparticle surface. In contrast, in the bulk-exchanged particles, the cross peaks were observed largely because of the

homogeneous mixing of the two ligands and hence extensive interactions between the neighboring ligand protons (Jackson et al. 2004, 2006).

Conclusion

In summary, Janus nanoparticles were prepared which took advantage of the interfacial exchange reactions of alkanethiolate-protected gold nanoparticles with mercapto-alcohols. Experimentally, Langmuir–Blodgett monolayers of the hydrophobic nanoparticles were immersed into an aqueous solution of the hydrophilic thiols. The reaction dynamics was then examined by contact angle measurements. At equilibrium, contact angle and spectroscopic studies indicated that about 50% of the original hydrophobic ligands were replaced with the hydrophilic ones, and the resulting particles exhibited segregated distribution of the two kinds of ligands, as confirmed by NOESY NMR measurements, supporting the amphiphilic structural model of the Janus nanoparticles. Additionally, because of the anisotropic characteristics of the Janus nanoparticle surface, extensive aggregation was also observed in selected solvent media. These asymmetric structural units might be further exploited for the controlled assembly into organized functional nanoarchitectures.

Acknowledgments This work was supported by a grant from the National Science Foundation (DMR-0804049) and the UC MEXUS-CONACYT program.

References

- Bella J, Borocci S, Mancini G (1999) Recognition in organized aggregates formed by a chiral amidic surfactant. *Langmuir* 15(23):8025–8031. doi:10.1021/la990277g
- Binks BP, Clint JH, Fletcher PDI, Lees TJG, Taylor P (2006) Growth of gold nanoparticle films driven by the coalescence of particle-stabilized emulsion drops. *Langmuir* 22(9):4100–4103. doi:10.1021/la052752i
- Bohren CF, Huffman DR (1983) Absorption and scattering of light by small particles. Wiley, New York
- Brauer G (1963) Handbook of preparative inorganic chemistry. Academic Press, New York
- Brust M, Walker M, Bethell D, Schiffrin DJ, Whyman R (1994) Synthesis of thiol-derivatized gold nanoparticles in a 2-phase liquid–liquid system. *J Chem Soc Chem Commun* (7):801–802. doi:10.1039/c39940000801
- Chen SW (2001a) Electrochemical studies of Langmuir–Blodgett thin films of electroactive nanoparticles. *Langmuir* 17(21):6664–6668. doi:10.1021/la0107042
- Chen SW (2001b) Langmuir–Blodgett fabrication of two-dimensional robust cross-linked nanoparticle assemblies. *Langmuir* 17(9):2878–2884. doi:10.1021/la001728w
- Emin SM, Denkova PS, Papazova KI, Dushkin CD, Adachi E (2007) Study of reverse micelles of di-isobutylphenoxy-ethoxyethylmethylbenzylammonium methacrylate in benzene by nuclear magnetic resonance spectroscopy. *J Colloid Interface Sci* 305(1):133–141. doi:10.1016/j.jcis.2006.08.013
- Feldheim DL, Grabar KC, Natan MJ, Mallouk TE (1996) Electron transfer in self-assembled inorganic polyelectrolyte/metal nanoparticle heterostructures. *J Am Chem Soc* 118(32):7640–7641. doi:10.1021/ja9612007
- Glotzer SC (2004) Materials science: some assembly required. *Science* 306(5695):419–420. doi:10.1126/science.1099988
- Guo Y, Moffitt MG (2007) Semiconductor quantum dots with environmentally responsive mixed polystyrene/poly(methyl methacrylate) brush layers. *Macromolecules* 40(16):5868–5878. doi:10.1021/ma070855x
- Guo R, Song Y, Wang GL, Murray RW (2005) Does core size matter in the kinetics of ligand exchanges of monolayer-protected Au clusters? *J Am Chem Soc* 127(8):2752–2757. doi:10.1021/ja044638c
- Hostetler MJ, Wingate JE, Zhong CJ, Harris JE, Vachet RW, Clark MR et al (1998) Alkanethiolate gold cluster molecules with core diameters from 1.5 to 5.2 nm: core and monolayer properties as a function of core size. *Langmuir* 14(1):17–30. doi:10.1021/la970588w
- Hostetler MJ, Templeton AC, Murray RW (1999) Dynamics of place-exchange reactions on monolayer-protected gold cluster molecules. *Langmuir* 15(11):3782–3789. doi:10.1021/la981598f
- Jackson AM, Myerson JW, Stellacci F (2004) Spontaneous assembly of subnanometre-ordered domains in the ligand shell of monolayer-protected nanoparticles. *Nat Mater* 3(5):330–336. doi:10.1038/nmat1116
- Jackson AM, Hu Y, Silva PJ, Stellacci F (2006) From homoligand- to mixed-ligand-monolayer-protected metal nanoparticles: a scanning tunneling microscopy investigation. *J Am Chem Soc* 128(34):11135–11149. doi:10.1021/ja061545h
- Kerker M (1969) The scattering of light, and other electromagnetic radiation. Academic Press, New York
- Kohlmann O, Steinmetz WE, Mao XA, Wuelfing WP, Templeton AC, Murray RW et al (2001) NMR diffusion, relaxation, and spectroscopic studies of water soluble, monolayer-protected gold nanoclusters. *J Phys Chem B* 105(37):8801–8809. doi:10.1021/jp011123o
- Morris KF, Froberg AL, Becker BA, Almeida VK, Tarus J, Larive CK (2005) Using NMR to develop insights into electrokinetic chromatography. *Anal Chem* 77(13):254A–263A
- Nie ZH, Li W, Seo M, Xu SQ, Kumacheva E (2006) Janus and ternary particles generated by microfluidic synthesis: design, synthesis, and self-assembly. *J Am Chem Soc* 128(29):9408–9412. doi:10.1021/ja060882n
- Nisisako T, Torii T, Takahashi T, Takizawa Y (2006) Synthesis of monodisperse bicolored Janus particles with electrical anisotropy using a microfluidic co-flow system. *Adv Mater* 18(9):1152–1156. doi:10.1002/adma.200502431

- Perro A, Reculosa S, Ravaine S, Bourgeat-Lami EB, Duguet E (2005) Design and synthesis of Janus micro- and nanoparticles. *J Mater Chem* 15(35–36):3745–3760. doi:[10.1039/b505099e](https://doi.org/10.1039/b505099e)
- Pradhan S, Xu LP, Chen SW (2007) Janus nanoparticles by interfacial engineering. *Adv Funct Mater* 17(14):2385–2392. doi:[10.1002/adfm.200601034](https://doi.org/10.1002/adfm.200601034)
- Song Y, Murray RW (2002) Dynamics and extent of ligand exchange depend on electronic charge of metal nanoparticles. *J Am Chem Soc* 124(24):7096–7102. doi:[10.1021/ja0174985](https://doi.org/10.1021/ja0174985)
- Storhoff JJ, Elghanian R, Mucic RC, Mirkin CA, Letsinger RL (1998) One-pot colorimetric differentiation of polynucleotides with single base imperfections using gold nanoparticle probes. *J Am Chem Soc* 120(9):1959–1964. doi:[10.1021/ja972332i](https://doi.org/10.1021/ja972332i)
- Takei H, Shimizu N (1997) Gradient sensitive microscopic probes prepared by gold evaporation and chemisorption on latex spheres. *Langmuir* 13(7):1865–1868. doi:[10.1021/la9621067](https://doi.org/10.1021/la9621067)
- Templeton AC, Wuelfing MP, Murray RW (2000) Monolayer protected cluster molecules. *Acc Chem Res* 33(1):27–36. doi:[10.1021/ar9602664](https://doi.org/10.1021/ar9602664)
- Ujihara M, Mitamura K, Torikai N, Imae T (2006) Fabrication of metal nanoparticle monolayers on amphiphilic poly(amido amine) dendrimer Langmuir films. *Langmuir* 22(8):3656–3661. doi:[10.1021/la053202n](https://doi.org/10.1021/la053202n)
- van Herrikhuyzen J, Portale G, Gielen JC, Christianen PCM, Sommerdijk NAJM, Meskers SCJ et al (2008) Disk micelles from amphiphilic Janus gold nanoparticles. *Chem Commun* 6:697–699. doi:[10.1039/b715820c](https://doi.org/10.1039/b715820c)
- Wang H, Brandl DW, Le F, Nordlander P, Halas NJ (2006a) Nanorice: a hybrid plasmonic nanostructure. *Nano Lett* 6(4):827–832. doi:[10.1021/nl060209w](https://doi.org/10.1021/nl060209w)
- Wang Y, Hernandez RM, Bartlett DJ, Bingham JM, Kline TR, Sen A et al (2006b) Bipolar electrochemical mechanism for the propulsion of catalytic nanomotors in hydrogen peroxide solutions. *Langmuir* 22(25):10451–10456. doi:[10.1021/la0615950](https://doi.org/10.1021/la0615950)
- Whetten RL, Khoury JT, Alvarez MM, Murthy S, Vezmar I, Wang ZL et al (1996) Nanocrystal gold molecules. *Adv Mater* 8(5):428–433. doi:[10.1002/adma.19960080513](https://doi.org/10.1002/adma.19960080513)
- Woehrlé GH, Warner MG, Hutchison JE (2004) Molecular-level control of feature separation in one-dimensional nanostructure assemblies formed by biomolecular nanolithography. *Langmuir* 20(14):5982–5988. doi:[10.1021/la049491h](https://doi.org/10.1021/la049491h)
- Xu LP, Pradhan S, Chen SW (2007) Adhesion force studies of Janus nanoparticles. *Langmuir* 23(16):8544–8548. doi:[10.1021/la700774g](https://doi.org/10.1021/la700774g)
- Zhang ZK, Cui ZL (1998) Catalytic functions of metal nanoparticles on polymerization of acetylene. *J Mar Sci Technol* 14(5):395–398